

Single image super-resolution via non-local normalized graph Laplacian regularization: A self-similarity tribute

Mehran Ebrahimi*, Sean Bohun

Faculty of Science, University of Ontario Institute of Technology, 2000 Simcoe Street North, Oshawa, Ontario, Canada, L1G 0C5



ARTICLE INFO

Article history:

Available online 28 August 2020

Keywords:

Super-resolution
Regularization
Image restoration
Image zooming
Graph laplacian
Self-similarity
Fractal-based restoration

ABSTRACT

The process of producing a high-resolution image given a single low-resolution noisy measurement is called single-frame image super-resolution (SISR). Historically, many fractal-based schemes have been proposed in the literature to address the SISR problem. Many conventional interpolation schemes fail to preserve important edge information of natural images and cannot be used blindly for resolution enhancement. Generally, *a-priori* constraints are required in the process of high resolution image approximation. We model the SISR problem as an energy minimization procedure which balances data fidelity and a regularization term. The regularization term will implicitly incorporate natural image redundancy via a normalized graph Laplacian operator, as a self-similarity based prior. This operator applies a non-local kernel similarity measure due to the choice of a non-local operator for the weight assignment. The data fidelity term is modelled as a likelihood estimator that is scaled using a sharpening term composed from the normalized graph Laplacian operator. Finally, a conjugate gradient scheme is used to minimize the objective functional. Promising results on resolution enhancement for a variety of digital images will be presented.

© 2020 Elsevier B.V. All rights reserved.

1. Introduction

The process of producing a high-resolution image given a single low-resolution noisy measurement is called single-frame image super-resolution (SISR). Many conventional interpolation schemes fail to preserve important edge information of natural images and cannot be used blindly for resolution enhancement. In SISR schemes, approximation of high-frequency image information is generally required to preserve edge-information and suppress noise. Many of the previously proposed SISR techniques [1–9] estimate missing high-resolution pixel information by making prior assumptions on the reconstructed image, as the high-resolution image is not known in advance. Historically, many fractal-based schemes have been proposed in the literature to address the SISR problem [7,8] by formulating self-similarity based priors.

Given a natural image, similarity between image patches represented by intensity values exists both within the same scale, as well as across scales in the image domain [7–17]. Self-similarity property of natural images has been utilized for a variety of image restoration tasks, including the Non-Local Means denoising method [18] and a variety of super-resolution algorithms in the spatial domain [2,7,8].

* Corresponding author.

E-mail addresses: mehran.ebrahimi@uoit.ca (M. Ebrahimi), sean.bohun@uoit.ca (S. Bohun).

Recently, a deblurring algorithm proposed by Kheradmand et al. [19] has shown promising results utilizing a new definition of the non-local normalized graph Laplacian operator as a regularization functional. In this manuscript, we adapt this regularization functional to solve the SISR problem.

In Section 2, we provide the mathematical model corresponding to the SISR problem. In Section 3, we review the graph-based image restoration model as discussed in [19]. We extend this model to SISR, in Section 4. Our experiments will be presented in Section 5, followed by conclusions in Section 6.

2. Mathematical model

We first describe the forward model corresponding to the Single Image Super-Resolution problem. The given Low-Resolution (LR) image of size $N \times M$, represented as a column vector $\underline{y} \in \mathbb{R}^{(NM) \times 1}$ is modelled as

$$\underline{y} = \mathbf{H}\underline{x} + \underline{n}_\sigma \quad (1)$$

where $\underline{x} \in \mathbb{R}^{(L^2 NM) \times 1}$ is the High-Resolution (HR) image of size $LN \times LM$ to be recovered. L is the zooming factor in each direction, $\mathbf{H} \in \mathbb{R}^{(NM) \times (L^2 NM)}$ is a degradation operator, and \underline{n}_σ a vector representing additive white Gaussian noise with standard deviation σ and 0 mean. For simplicity, we assume that both LR measurement \underline{y} and the HR image \underline{x} are square images, i.e., $N = M$.

Problem: Given a single low resolution measurement \underline{y} and degradation operator $\mathbf{H} = \mathbf{D}\mathbf{B}$ as a composition of blur \mathbf{B} followed by down-sampling operator \mathbf{D} , we wish to find a high-resolution image \underline{x} that minimizes

$$S(\cdot, \underline{y}) = \operatorname{argmin}_{\underline{x}} (\mathcal{D}(\underline{y}, \underline{x}) + \mathcal{R}(\underline{y}, \underline{x})) \quad (2)$$

where \mathcal{D} , the data fidelity term, attempts to ensure that the blurred, decimated \underline{x} will be consistent with the given measurement \underline{y} . Furthermore, the regularization term \mathcal{R} imposes feasibility constraints on \underline{x} .

3. Graph-based image restoration

There have been a variety of successful image restoration algorithms derived according to a graph-based approach [20]. We first review the concept of non-local normalized graph Laplacian according to Kheradmand et al. [19]. This operator is composed according to the non-local “interactions” of neighbouring pixels.

An image is defined as an intensity function \underline{x} on vertices V of a weighted graph $G = G(V, E, K)$ consisting of a triplet that includes:

1. A set of vertices V (image pixels);
2. A collection of edges $E \subset V \times V$;
3. A set of weights $K(u, v)$ on edges connecting the vertices that describe similarity between two vertices.

The composition of the normalized graph Laplacian requires a similarity measure to compute edge weights K , which in turn describes the underlying structure of the image. A choice for the similarity measure of the normalized graph Laplacian operator according to [19] is based on the weights introduced in the Non-Local Means (NLM) denoising algorithm [18]. Given the (u, v) edge, the Non-local similarity measure is given by

$$K(u, v) = \exp \left(-\frac{\|\tilde{\underline{y}}_u - \tilde{\underline{y}}_v\|^2}{h^2} \right) \quad (3)$$

where $\tilde{\underline{y}}_u$ is the patch surrounding the pixel u of \underline{y} and $\tilde{\underline{y}}_v$ is the patch surrounding v . Finally h is a smoothing parameter.

Given the similarity matrix K , a diagonal scaling matrix C is computed according to the Sinkhorn-Knopp (SK) algorithm, an iterative method which rescales all rows and columns of a given matrix to sum-up to 1 [19]. Normalizing the matrix K using C results in the filtering matrix W given by

$$W = C^{-\frac{1}{2}} K C^{-\frac{1}{2}}$$

which is doubly stochastic, symmetric, and positive definite [19]. This operator has beneficial spectral properties for image processing purposes. Decomposing the filtering matrix as $W = \Gamma\Gamma^T$ where Γ is the orthonormal matrix with columns representing the eigenvectors of filtering matrix W and $J = \operatorname{diag}\{\lambda_1, \lambda_2, \dots, \lambda_{N^2}\}$ includes the corresponding eigenvalues. Since the filtering matrix W is doubly stochastic, associated eigenvalues follow $\lambda_1 = 1 > \lambda_2 \geq \dots \geq \lambda_{N^2} \geq 0$, implying that largest eigenvalue is exactly equal to one with corresponding eigenvector $\mathbf{v}_1 = (\frac{1}{\sqrt{N^2}})(\mathbf{1}_{N^2})^T$, [19]. This is a favorable property since it ensures the preservation of DC component of signal after applying the filtering matrix W [21].

We define the normalized graph Laplacian operator as $I - W$, [21]. Furthermore, the proposed regularization functional is formed as

$$\mathcal{R}(\underline{x}) = \eta \underline{x}^T (I - W) \underline{x}. \quad (4)$$

Data fidelity term \mathcal{D} is represented as a “sharpened” likelihood function

$$\mathcal{D}(\underline{y}, \underline{x}) = (\underline{y} - \mathbf{H}\underline{x})^T (I + \beta(I - W)) (\underline{y} - \mathbf{H}\underline{x})$$

which acts as a sharpening filter on residuals of $\underline{y} - \mathbf{H}\underline{x}$ since matrix $I - W$ behaves similar to a high pass filter [19]. Given the composition of the graph Laplacian operator, the components of the deblurring function proposed by the authors of [19] is given by

$$E(\cdot, \underline{y}) = \operatorname{argmin}_{\underline{x}} \left((\underline{y} - \mathbf{H}\underline{x})^T (I + \beta(I - W)) (\underline{y} - \mathbf{H}\underline{x}) + \eta \underline{x}^T (I - W) \underline{x} \right) \quad (5)$$

with respect to unknown vector \underline{x} where matrix $K = K(u, v)$ measures similarity between edges $\{u, v\}$, \mathbf{H} a symmetric blur operator and C a diagonal scaling matrix. Parameters η and β are tuned depending on the amount of noise and blur of measurement \underline{y} . The above objective functional in Eq. (5) is then converted to a corresponding linear system of equations, and is solved using Conjugate Gradient algorithm. Once the above objective is minimized, a deblurred version \underline{x} of measurement \underline{y} will be produced.

We now explain how to adapt the non-local normalized graph Laplacian operator to solve our SISR inverse problem.

4. Normalized graph Laplacian operator for super-resolution

We introduce the new objective function for the SISR inverse problem as

$$S(\underline{y}) = \operatorname{argmin}_{\underline{x}} (\underline{y} - \mathbf{H}\underline{x})^T (I_S + \beta(I_S - W_S)) (\underline{y} - \mathbf{H}\underline{x}) + \eta \underline{x}^T (I_L - W_L) \underline{x} \quad (6)$$

which once minimized, will produce the high resolution image \underline{x} given the single low resolution measurement \underline{y} . As before, the terms β and η are tuning parameters, matrix $\mathbf{H} = \mathbf{DB}$ is a degradation operator, finally W_S and W_L are filtering matrices that will be explained below.

We clarify the dimension and role of each term in the energy function in Eq. (6) in Table 1 for a zooming factor of L . It can be observed that as opposed to the deblurring energy functional (5) in [19], here we need different filtering matrix W in the objective functional to conform the matrix sizes matching the zooming factor. As a result new matrices W_S and W_L will be defined. The steps to find the filtering matrix W_L are:

1. Given LR image \underline{y} , estimate the standard deviation of noise σ ;
2. Denoise \underline{y} using the Block Matching 3D (BM3D) denoising algorithm [22];
3. Interpolate the denoised \underline{y} using any standard interpolation method by a factor of L to obtain a simulated high-resolution (HR) image \underline{y}_L ;
4. Compute filtering matrix W_L in the same fashion as W , using the simulated HR image \underline{y}_L .

The filtering matrix W_S calculated for the data fidelity term is computed after denoising \underline{y} and without any interpolation, similar to the deblurring objective in the previous section.

Recall that the energy function we wish to minimize includes regularization and fidelity functionals as

$$S(\underline{y}) = \operatorname{argmin}_{\underline{x}} (\underline{y} - \mathbf{H}\underline{x})^T (I_S + \beta(I_S - W_S)) (\underline{y} - \mathbf{H}\underline{x}) + \eta \underline{x}^T (I_L - W_L) \underline{x} \quad (7)$$

where W_S and W_L are filtering matrices in data fidelity and regularization terms respectively, \underline{y} is the low resolution measurement, \underline{x} is the high resolution solution, and $\mathbf{H} = \mathbf{DB}$ is the degradation operator. Finally, β and η are tuning parameters.

Table 1

Dimension of each term composing the proposed objective function (6) under the assumption that images are square and in lexicographical format with a decimation (zooming) factor of L .

Term	Role	Dimension
\underline{y}	Associated with input	$N^2 \times 1$
\mathbf{D}	Decimation operator	$N^2 \times (NL)^2$
\mathbf{B}	Blurring operator	$(NL)^2 \times (NL)^2$
$\mathbf{H} = \mathbf{DB}$	Degradation operator	$N^2 \times (NL)^2$
β	Associated with data fidelity \mathcal{D}	1×1
I_S	Tuning parameter	$N^2 \times N^2$
W_S	Identity matrix	$N^2 \times N^2$
η	Filtering matrix for \mathcal{D}	$N^2 \times N^2$
I_L	Associated with regularization \mathcal{R}	1×1
W_L	Identity matrix	$(NL)^2 \times (NL)^2$
\underline{x}	Filtering matrix for \mathcal{R}	$(NL)^2 \times (NL)^2$
	Associated with output	$(NL)^2 \times 1$
	Reconstructed HR estimate	$(NL)^2 \times 1$

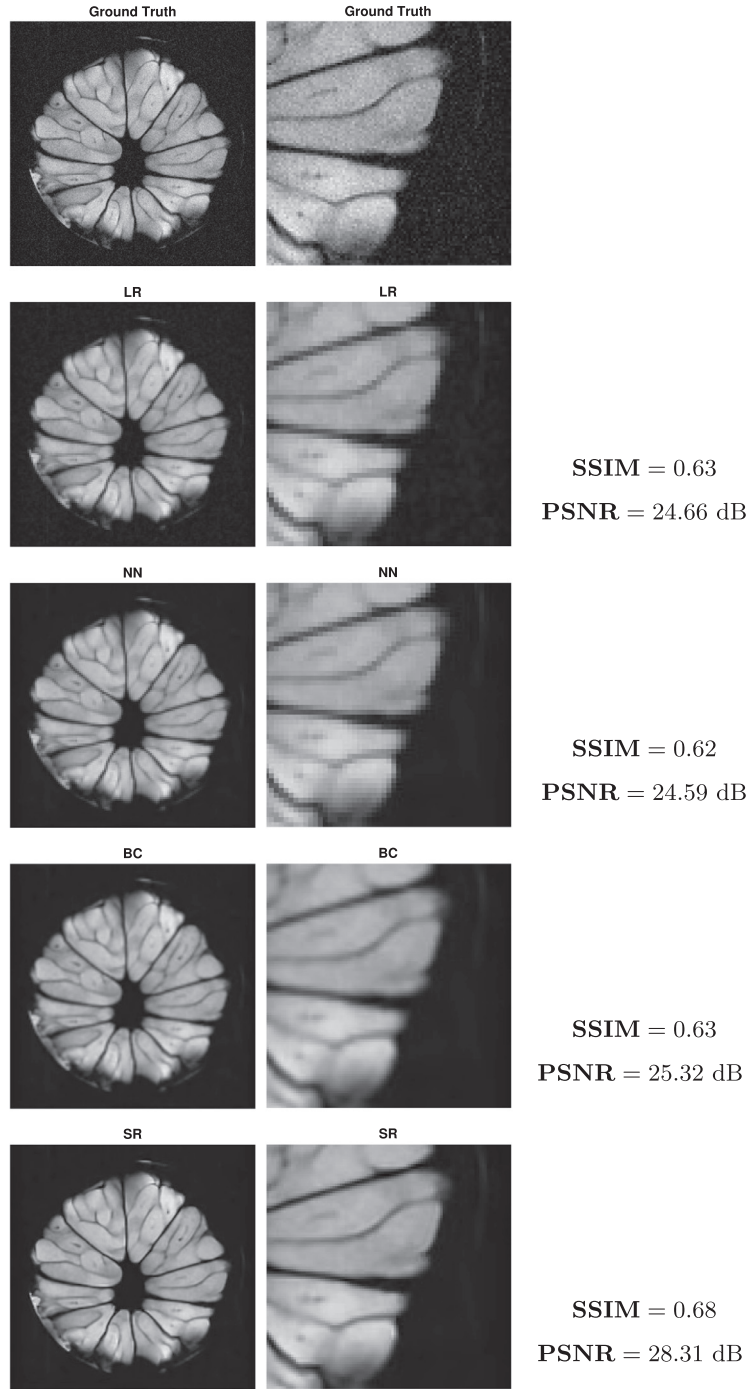


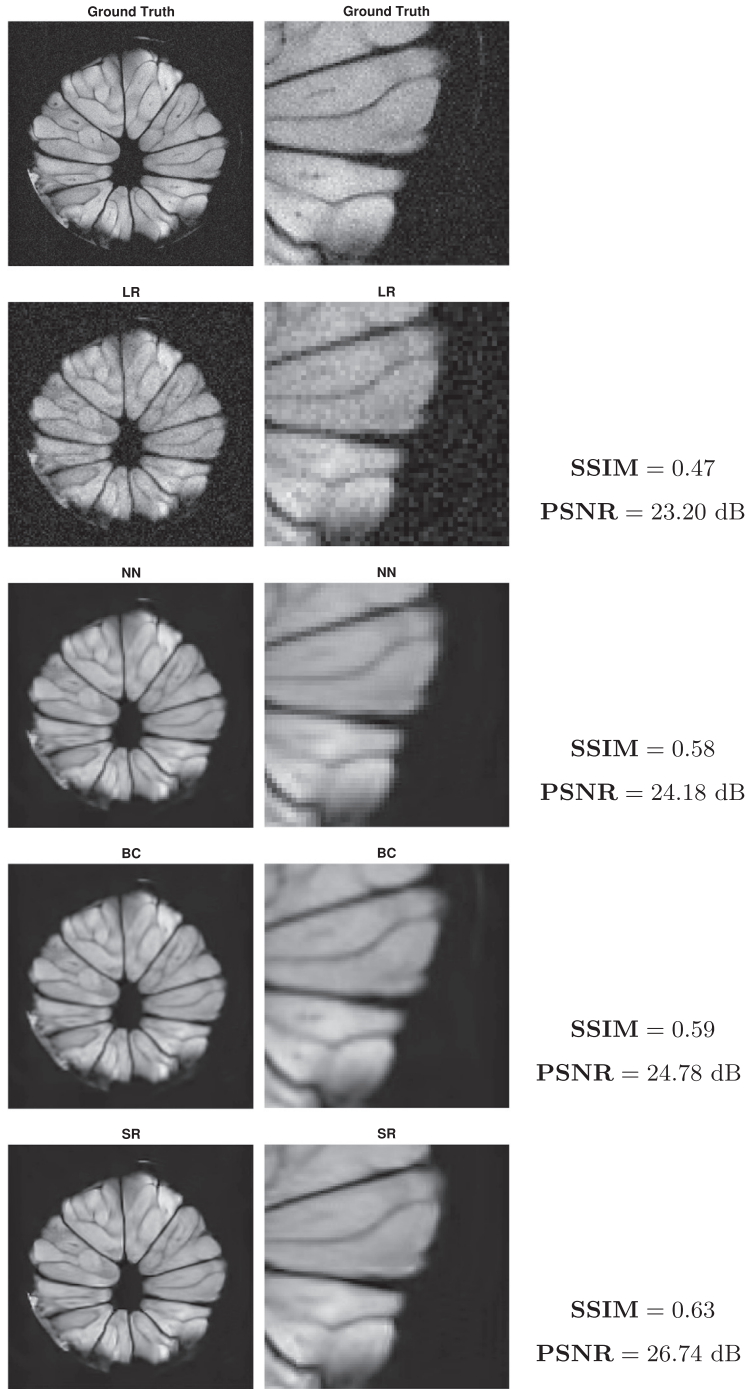
Fig. 1. Lime data with $\sigma = 0$.

We can simplify this energy function using the following change of variables

$$\mathbf{P} = I_S + \beta(I_S - W_S), \quad \mathbf{Q} = \eta(I_L - W_L).$$

Using these change of variables and considering that \mathbf{P} is symmetric, the objective functional to be minimized in Eq. (7) can be written as

$$\begin{aligned} S(\underline{x}, \underline{y}) &= (\underline{y} - \mathbf{H}\underline{x})^T \mathbf{P} (\underline{y} - \mathbf{H}\underline{x}) + \underline{x}^T \mathbf{Q} \underline{x} \\ &= \underline{y}^T \mathbf{P} \underline{y} - (\underline{y}^T \mathbf{P} \mathbf{H} \underline{x})^T - \underline{x}^T \mathbf{H}^T \mathbf{P}^T \underline{y} + \underline{x}^T \mathbf{H}^T \mathbf{P} \mathbf{H} \underline{x} + \underline{x}^T \mathbf{Q} \underline{x} \end{aligned}$$

**Fig. 2.** Lime data with $\sigma = 10$.

$$\begin{aligned}
 &= \underline{y}^T \mathbf{P} \underline{y} - \underline{x}^T \mathbf{H}^T \mathbf{P}^T \underline{y} - \underline{x}^T \mathbf{H}^T \mathbf{P}^T \underline{y} + \underline{x}^T \mathbf{H}^T \mathbf{P} \mathbf{H} \underline{x} + \underline{x}^T \mathbf{Q} \underline{x} \\
 &= \underline{y}^T \mathbf{P} \underline{y} - 2\underline{x}^T \mathbf{H}^T \mathbf{P}^T \underline{y} + \underline{x}^T \mathbf{H}^T \mathbf{P} \mathbf{H} \underline{x} + \underline{x}^T \mathbf{Q} \underline{x}
 \end{aligned} \tag{8}$$

where $\underline{y}^T \mathbf{P} \mathbf{H} \underline{x}$ is a 1×1 matrix, and therefore equals its own transpose as a scalar. Taking the gradient of the objective function S that we wish to minimize in expression (8) and setting $\nabla_{\underline{x}} S = \underline{0}$ yields

$$-2\mathbf{H}^T \mathbf{P}^T \underline{y} + 2\mathbf{H}^T \mathbf{P} \mathbf{H} \underline{x} + 2\mathbf{Q} \underline{x} = \underline{0}.$$

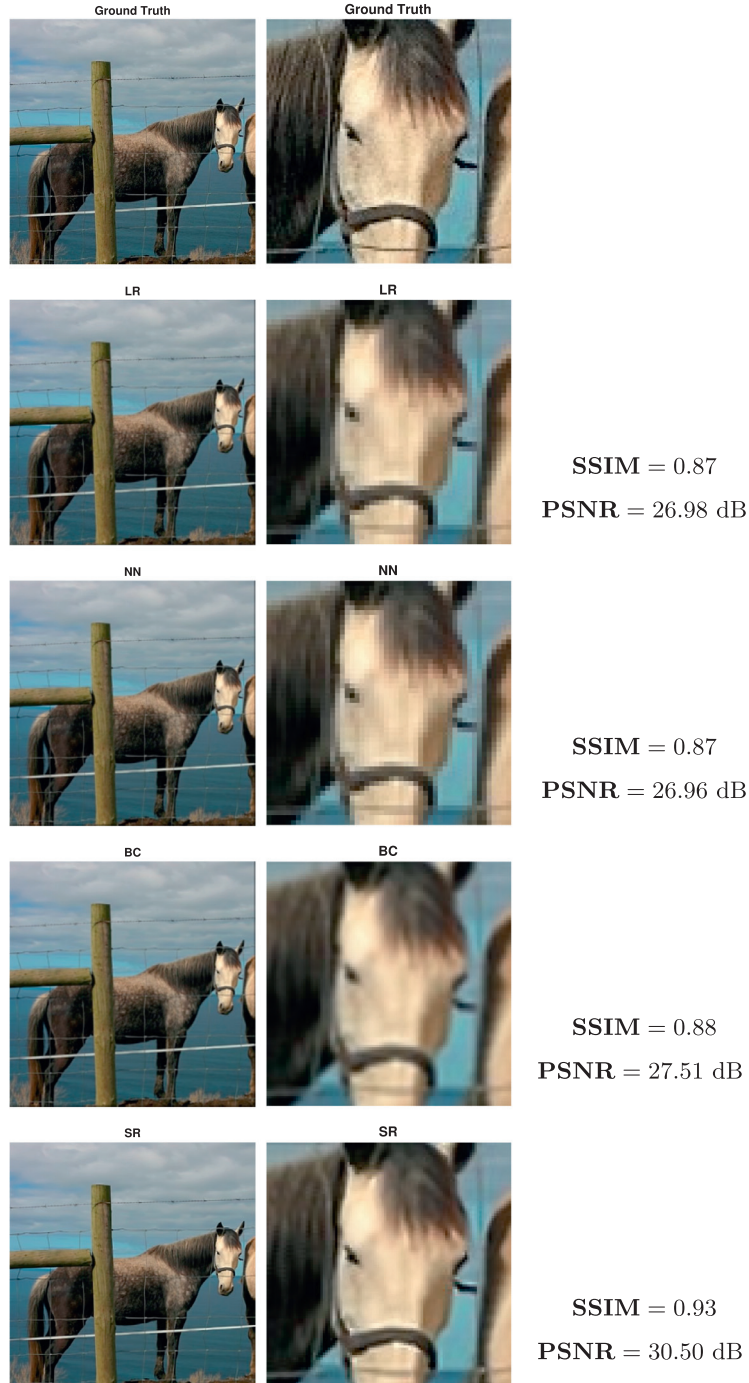


Fig. 3. Horses data with $\sigma = 0$.

The result is a positive definite system of equations $(\mathbf{H}^T \mathbf{P} \mathbf{H} + \mathbf{Q}) \underline{x} = \mathbf{H}^T \mathbf{P}^T \underline{y}$, and solving for \underline{x} yields

$$\underline{x} = (\mathbf{H}^T \mathbf{P} \mathbf{H} + \mathbf{Q})^{-1} \mathbf{H}^T \mathbf{P}^T \underline{y}. \quad (9)$$

We solve this system of linear equations using the conjugate gradient iterative scheme with an initial input $\underline{x}_0 \in \mathbb{R}^{(LN)^2 \times 1}$, defined as an interpolated denoised version of the low resolution input image \underline{y} .



Fig. 4. Horse data with $\sigma = 10$.

5. Experiments

Performance of the proposed algorithm is tested on a series of images. For colour images, each (RGB) channel is solved independently and then merged to form a restored final estimate \underline{x} . In all of these experiments, the blur operator \mathbf{B} represents local averaging blur followed by down-sampling operator \mathbf{D} , see [23].

We quantify the performance of our restoration algorithm with two measurements, the Peak Signal-to-Noise Ratio (PSNR) and Structural Similarity Index Measure (SSIM). We analyze the effects of varying the standard deviation of additive white

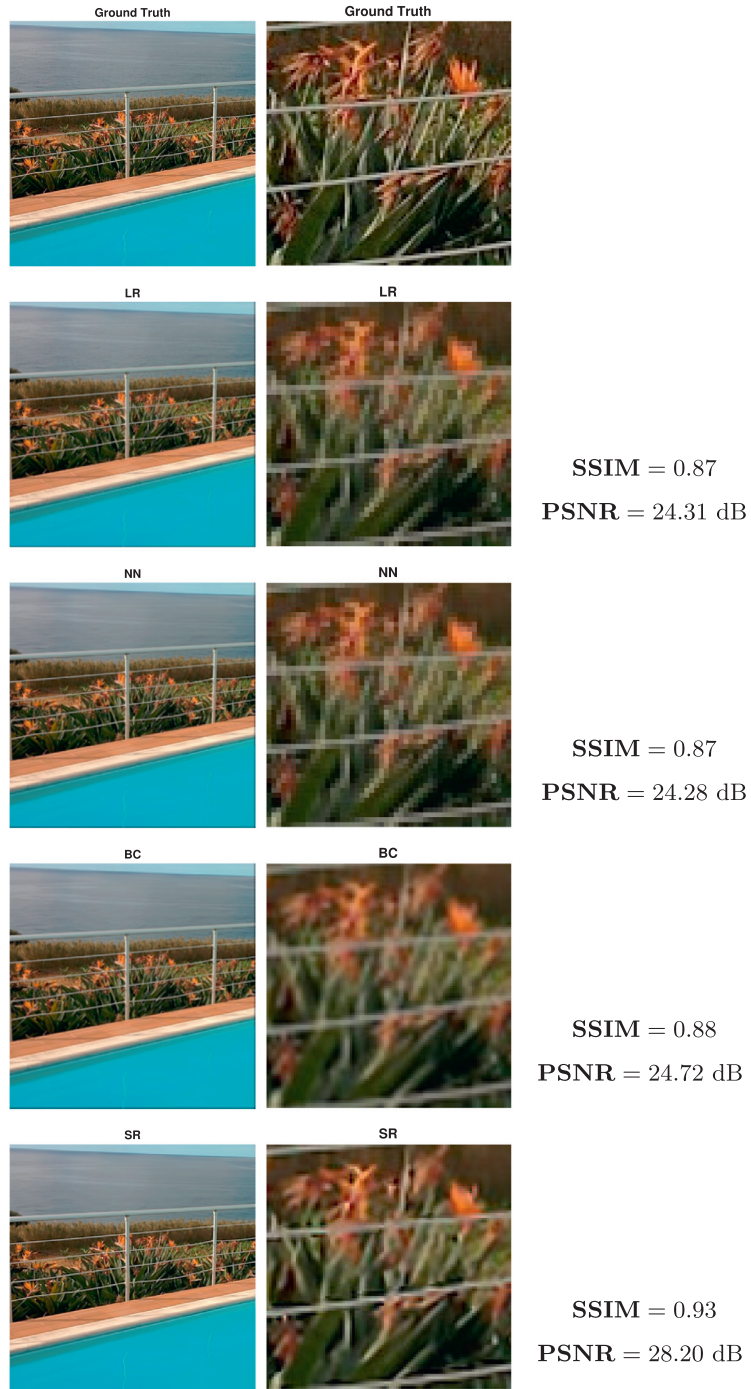


Fig. 5. Pool data with $\sigma = 0$.

Gaussian noise to our synthetic low resolution measurement $\underline{y} = \mathbf{H}\underline{x} + \underline{n}_\sigma$, such that the measurement will be degraded with either no noise ($\sigma = 0$) or a “moderate” amount of noise ($\sigma = 10$).

In the following set of experiments, all images are square and decimation factor $L = 2$ is used. Tuning parameters β and η are varied and adjusted, ensuring that β is chosen such that filtering matrix W is doubly stochastic and $\eta > 0$ to ensure penalization of the energy functional, here we choose $\eta = 0.1$ and $\beta = 1$.

The search window size for pixels considered a neighbouring pixel is set to 11×11 . In addition the intensity gray level vector patch size is set to be 5×5 . The boundary conditions imposed surrounding the search window are symmetric.

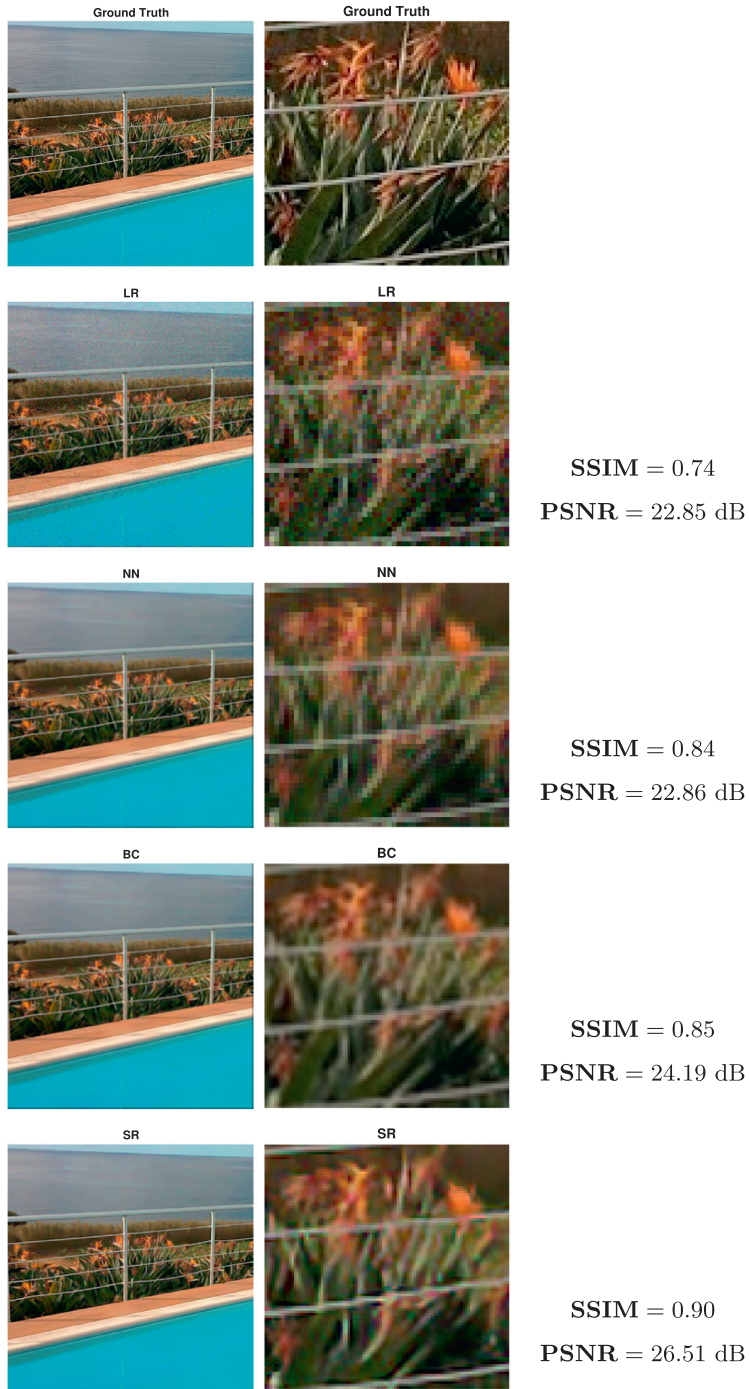
**Fig. 6.** Pool data with $\sigma = 10$.

Table 2 includes the PSNR and SSIM results for some test images where LR corresponds to Low Resolution input, Near-est Neighbor (NN) and BiCubic (BC) interpolation are used after an initial BM3D denoising. SR relates to the result of the proposed algorithm. We present some of the results relating to data for qualitative comparison in Figs. 1–8. “Lime” is a sample of lime fruit image scanned in a magnetic resonance imaging (MRI) scanner taken from [7], and the other images have been captured using a digital camera. It can be observed that our proposed SISR reconstruction algorithm outperforms interpolation schemes both qualitatively and quantitatively, in presence and without presence of additive noise.

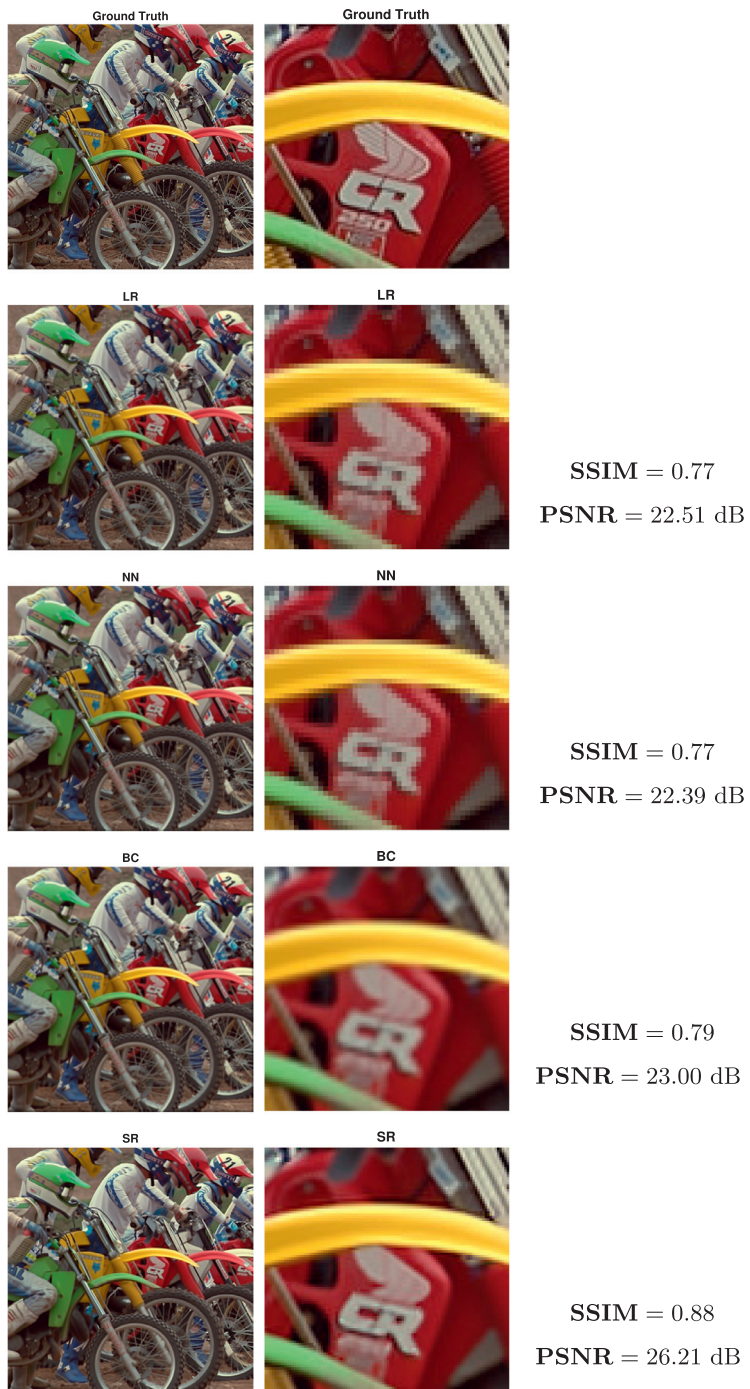


Fig. 7. Motorcycle data with $\sigma = 0$.

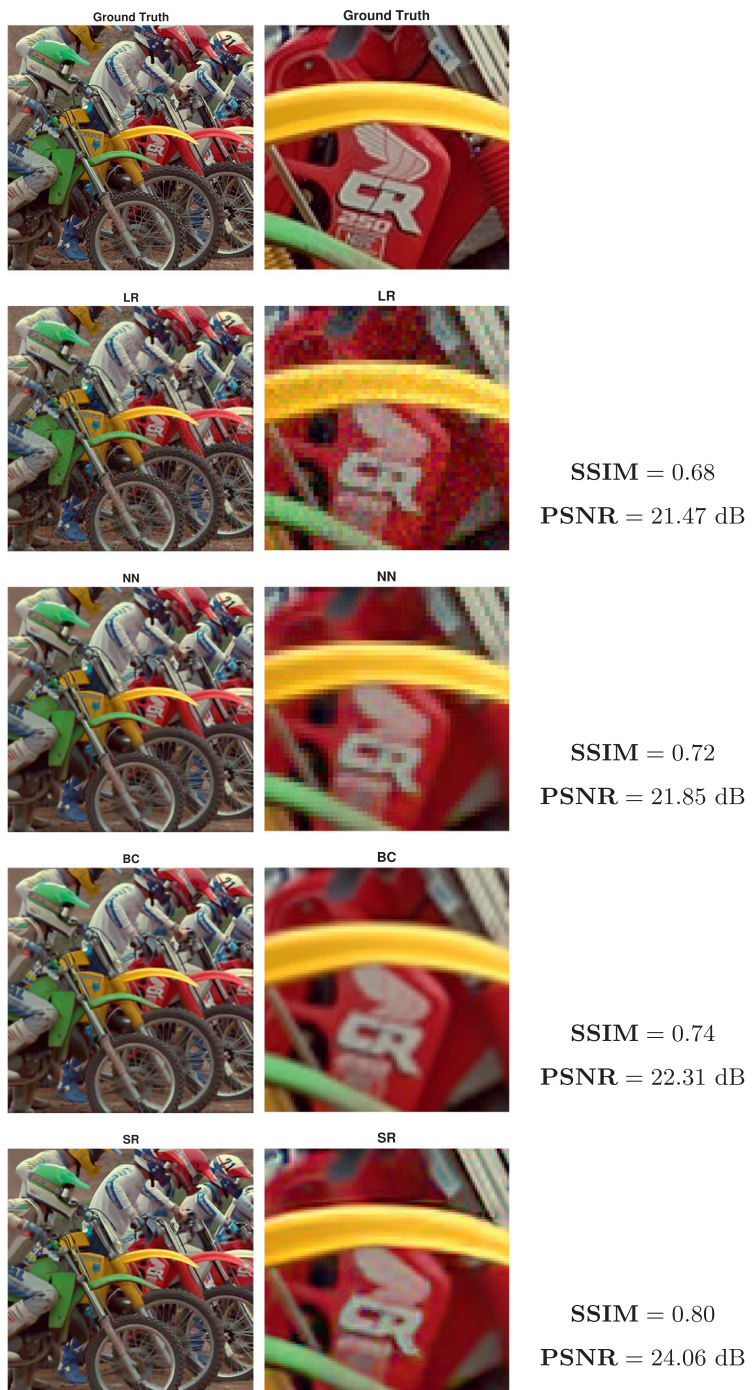


Fig. 8. Motorcycle data with $\sigma = 10$.

Table 2

Performance of the algorithm for various images for no noise, i.e. $\sigma = 0$ (top), and with additive white Gaussian noise with standard deviation $\sigma = 10$ (bottom).

Image		LR	NN	BC	SR
Motorcycle	PSNR (dB)	22.51	22.39	23.00	26.21
	SSIM	0.77	0.77	0.79	0.88
Pineapple	PSNR (dB)	20.31	20.23	20.58	22.70
	SSIM	0.63	0.62	0.63	0.75
Pool	PSNR (dB)	24.31	24.28	24.72	28.20
	SSIM	0.87	0.87	0.88	0.93
Horses	PSNR (dB)	26.98	26.96	27.51	30.50
	SSIM	0.87	0.87	0.88	0.93
Boat	PSNR (dB)	24.79	24.74	25.20	28.04
	SSIM	0.84	0.84	0.85	0.91
Lime	PSNR (dB)	24.66	24.59	25.32	28.31
	SSIM	0.63	0.62	0.63	0.68
Image		LR	NN	BC	SR
Motorcycle	PSNR (dB)	21.47	21.85	22.31	24.06
	SSIM	0.68	0.72	0.74	0.80
Pineapple	PSNR (dB)	19.67	19.85	20.14	21.52
	SSIM	0.55	0.57	0.58	0.68
Pool	PSNR (dB)	22.85	22.86	24.19	26.51
	SSIM	0.74	0.84	0.85	0.90
Horses	PSNR (dB)	24.53	26.34	26.75	28.51
	SSIM	0.67	0.83	0.84	0.87
Boat	PSNR (dB)	23.15	24.14	24.48	26.04
	SSIM	0.69	0.80	0.81	0.85
Lime	PSNR (dB)	23.20	24.18	24.78	26.74
	SSIM	0.47	0.58	0.59	0.63

6. Concluding remarks

We applied the normalized graph Laplacian operator to address the single image super-resolution problem. We presented a new mathematical model and numerical technique based on conjugate gradient minimization. The results were evaluated on various data both quantitatively and qualitatively. The technique seems to work best for images with least additive noise. We only considered examples where a local averaging operator was used for the blurring kernel. Our proposed technique can be extended to other blurring kernels and higher zooming factors.

Declaration of Competing Interest

None.

CRediT authorship contribution statement

Mehran Ebrahimi: Conceptualization, Methodology, Software, Validation, Formal analysis, Writing - original draft, Writing - review & editing, Funding acquisition. **Sean Bohun:** Writing - review & editing, Funding acquisition.

Acknowledgments

This research was supported in part by the Natural Sciences and Engineering Research Council of Canada (NSERC).

Mehran Ebrahimi would like to dedicate this work to Prof. Edward Vrscay of the University of Waterloo. Thank you for allowing me to be your doctoral student during 2003–2008, Ed. I am always thankful that you exposed me to the world of fractals, self-similarity, and mathematical imaging!

References

- [1] Nguyen NX. Numerical algorithms for image superresolution. Graduate program in scientific computation and computational mathematics, Stanford University; 2000. Ph.D. thesis.
- [2] Makwana RR, Mehta ND. Survey on Single image Super Resolution Techniques. IOSR J Electron Commun Eng 2013;5(5):23–33.
- [3] Freeman WT, Jones TR, Pasztor EC. Example-based super-resolution. IEEE Comput Graph Appl 2002;22(2):56–65.
- [4] Elad M, Datsenko D. Example-based regularization deployed to super-resolution reconstruction of a single image. Comput J 2007;50(4):1–16.
- [5] Farsiu S, Robinson D, Elad M, Milanfar P. Advances and challenges in super-resolution. Int J Imaging Syst Technol 2004;14(2):47–57.
- [6] Chaudhuri S. Super-resolution imaging. Boston, MA: Kluwer; 2001.
- [7] Ebrahimi M, Vrscay ER. Solving the inverse problem of image zooming using self-examples. In: International conference image analysis and recognition. Springer; 2007. p. 117–30.

- [8] Ebrahimi M, Vrscay ER. Multi-frame super-resolution with no explicit motion estimation; 2008. p. 455–9.
- [9] Glasner D, Bagon S, Irani M. Super-resolution from a single image. In: 2009 IEEE 12th International conference on computer vision (ICCV). IEEE; 2009. p. 349–56.
- [10] Ebrahimi M. Inverse problems and self-similarity in imaging. University of Waterloo; 2008. Ph.D. thesis.
- [11] La Torre D, Vrscay ER, Barnsley MF. Measure-valued images, associated fractal transforms, and the affine self-similarity of images. SIAM J. Imaging Sci. 2009;2(2):470–507.
- [12] Ebrahimi M, Vrscay ER. Nonlocal-means single-frame image zooming. In: PAMM: Proceedings in applied mathematics and mechanics, vol. 7. Wiley Online Library; 2007. p. 2020067–8.
- [13] Ebrahimi M, Vrscay ER. Regularized fractal image decoding. In: 2006 Canadian conference on electrical and computer engineering. IEEE; 2006. p. 1964–9.
- [14] Ebrahimi M, Vrscay ER. Fractal image coding as projections onto convex sets. In: International conference image analysis and recognition. Springer; 2006. p. 493–506.
- [15] Ebrahimi M, Vrscay ER. Regularization schemes involving self-similarity in imaging inverse problems. In: Journal of physics: conference series, 124. IOP Publishing; 2008. p. 012021.
- [16] Ebrahimi M, Vrscay ER. Self-similarity in imaging 20 years after fractals everywhere. In: International workshop on local and non-local approximation in image processing (LNLA); 2008. p. 165–72.
- [17] Ebrahimi M, Vrscay ER. Examining the role of scale in the context of the non-local-means filter. In: International conference image analysis and recognition. Springer; 2008. p. 170–81.
- [18] Buades A, Coll B, Morel J-M. A non-local algorithm for image denoising. In: Proceedings of IEEE conference on computer vision and pattern recognition (CVPR), 2; 2005. p. 60–5. doi:[10.1109/CVPR.2005.38](https://doi.org/10.1109/CVPR.2005.38).
- [19] Kheradmand A, Milanfar P. A general framework for regularized, similarity-based image restoration. IEEE Trans Image Process 2014;23(12):5136–51. doi:[10.1109/TIP.2014.2362059](https://doi.org/10.1109/TIP.2014.2362059).
- [20] Shuman DI, Narang SK, Frossard P, Ortega A, Vandergheynst P. The emerging field of signal processing on graphs: extending high-dimensional data analysis to networks and other irregular domains. IEEE Signal Process Mag 2013;30(3):83–98. doi:[10.1109/MSP.2012.2235192](https://doi.org/10.1109/MSP.2012.2235192).
- [21] Milanfar P. Symmetrizing smoothing filters. SIAM J. Imaging Sci. 2013;6(1):263–84. doi:[10.1137/120875843](https://doi.org/10.1137/120875843).
- [22] Dabov K, Foi A, Katkovnik V, Egiazarian K. Image denoising with block-matching and 3d filtering. In: Image processing: algorithms and systems, neural networks, and machine learning, vol. 6064. International Society for Optics and Photonics; 2006. p. 606414.
- [23] Ebrahimi M, Vrscay ER, Martel AL. Coupled multi-frame super-resolution with diffusive motion model and total variation regularization. In: 2009 International workshop on local and non-local approximation in image processing. IEEE; 2009. p. 62–9.